Environmental Science Nano

ROYAL SOCIETY OF CHEMISTRY

PAPER

View Article Online
View Journal | View Issue

Cite this: *Environ. Sci.: Nano*, 2023, **10**, 2286

Graphene oxide degradation by a white-rot fungus occurs in spite of lignin peroxidase inhibition†

Lorenzo Fortuna,[a] Marina Garrido,‡[b] Humberto Castillo-Gonzalez,[b] Davide Zanelli,[c] Cristina Martín,§[d] Fabio Candotto Carniel,*[c] Ester Vázquez,[ef] Maurizio Prato,[bgh] Alberto Bianco[d] and Mauro Tretiach[c]

This study investigated the degradation of graphene oxide (GO) by the white-rot fungus *Phanerochaete chrysosporium*. Axenic fungal suspensions were inoculated in malt extract glucose medium enriched with various concentrations of GO and allowed to grow for several months. Biomass, pH, H_2O_2 content and activity of laccase (Lac) and lignin peroxidase (LiP) in the culture media were monitored, along with the physicochemical changes of GO over time followed by TEM, Raman, XPS and TGA. Lower concentrations of GO exhibited a stronger stimulating effect on *P. chrysosporium* growth and the production of Lac and H_2O_2 compared to higher concentrations, probably due to an excessive parallel increase in GO degradation by-products. The fungus significantly altered the structure of GO, with increase in the Raman D band, although GO neutralized LiP activity, possibly by unspecific adsorption. The activity of isolated LiP, but not of Lac, was suppressed in the presence of GO. Moreover, Lac caused modifications in the GO lattice as evidenced by a significant increase in the ratio between the intensity of the D and G bands of the Raman spectra. This enzyme emerges as a key player in the biodegradation of GRMs within terrestrial ecosystems, as its release extends beyond fungi to several other microorganisms.

Received 3rd February 2023,
Accepted 2nd July 2023

DOI: 10.1039/d3en00072a

rsc.li/es-nano

Environmental significance

The biodegradability of graphene-related materials (GRMs) is a key property for predicting their fate and impact in the environment, but it is still largely unknown. In a previous study we showed that white-rot and saprotrophic fungi are capable of degrading few-layer graphene (FLG) to a graphene oxide (GO)-like material. In this work we show that the white-rot fungus *Phanerochaete chrysosporium* can degrade GO, here used as a surrogate of the GO-like material. The degradation is not carried out by lignin peroxidase, the most reactive lignin-modifying enzyme which is restricted to white-rots and a few other microorganisms, but by laccases, biodegradative enzymes shared by all kingdoms of life. This finding averts the hypothesis of a possible GRM accumulation in terrestrial environments.

Introduction

Graphene is a carbon-based nanomaterial, which has attracted massive attention from academic researchers and technological industries for its extraordinary physical, mechanical, and electronic properties.[1,2] After its isolation in 2004,[3] several graphene-related materials (GRMs) have been developed. To date, FLG,[4] GO[5] and rGO[6] are the most used GRMs in numerous application fields, from optoelectronics to energy storage, to medicine. Nowadays, new graphene-

[a] *Department of Engineering and Architecture, University of Trieste, Trieste, Italy*
[b] *Department of Chemical and Pharmaceutical Sciences, University of Trieste, Trieste, Italy*
[c] *Department of Life Sciences, University of Trieste, Trieste, Italy. E-mail: fcandotto@units.it*
[d] *CNRS, Immunology, Immunopathology and Therapeutic Chemistry, UP3572, ISIS, University of Strasbourg, 67000 Strasbourg, France*
[e] *Facultad de Ciencias y Tecnologías Químicas, Universidad de Castilla-La Mancha, Ciudad Real, Spain*
[f] *Instituto Regional de Investigación Científica Aplicada (IRICA), Universidad de Castilla-La Mancha, Ciudad Real, Spain*
[g] *Center for Cooperative Research in Biomaterials (CIC biomaGUNE), Basque Research and Technology Alliance (BRTA), Paseo de Miramón 182, Spain*
[h] *Basque Foundation for Science, Ikerbasque, Bilbao, Spain*

† Electronic supplementary information (ESI) available. See DOI: https://doi.org/10.1039/d3en00072a

‡ Current address: IMDEA Nanociencia, Ciudad Universitaria de Cantoblanco, Madrid, Spain.
§ Current address: Department of Bioengineering, Universidad Carlos III de Madrid, Leganés, Spain.

based devices[7] and graphene-enriched materials (*e.g.* engineered plastics,[8] geopolymers,[9]) are reaching people's everyday life. During their life cycle, most of these materials will inevitably wear out, while others will not be properly disposed of, causing an involuntary release of GRMs and GRM-enriched particles into the environment. Besides, applications involving a deliberate release of GRMs in agricultural crops as pest controls,[10] drug carriers or fertilizers[11] have been developed. Therefore, there is increasing interest in understanding if the inadvertent or voluntary release of GRMs might represent a serious threat to biota and/or the ecosystem services they sustain.

Only a few studies have addressed the environmental fate of GRMs and, in particular, the paramount process of biodegradation by soil decomposers.[7,12,13] Among the organisms tested so far, fungi have proven to be the most effective.[7,13] Their degradation capability derives from the production and release of a plurality of oxidative enzymes, the so-called lignin modifying enzymes (LMEs), which include lignin peroxidase (LiP), Mn-peroxidase and laccase (Lac), in addition to their substrates (*e.g.* H_2O_2) and surfactants.[14,15] This enzymatic exudate, used to acquire organic molecules from dead organic matter,[16] can oxidize recalcitrant biomolecules such as lignin, but also xenobiotics such as polycyclic aromatic hydrocarbons (PAHs) and polychlorinated biphenyls (PCBs),[17,18] through the formation of radical species.[19] It has been already reported that isolated LMEs *in vitro* or white-rot fungi in GRM-enriched media are able to modify some GRMs [FLG flakes;[13] GO and rGO nanoribbons (NRs);[20] rGO flakes[7]]. However, these modifications fall short of the complete degradation documented by human myeloperoxidases.[21,22] Interestingly, recent studies demonstrated that the fungal degradation by-products derived from FLG have a structure very similar to that of GO.[13] GO is particularly reactive, due to the oxygenated functional groups bound to the graphene lattice, and it is thus potentially more toxic than other GRMs.[23] Therefore, it is crucial to determine if it can be further degraded by soil decomposers.

The effects of GO and other GRMs on fungal decomposers and their oxidative enzymes are controversial. On the one hand, the presence of rGO seems to enhance the growth of the white-rot fungus *Phanerochaete chrysosporium* (Fr.) P. Karst;[24] on the other hand, in the mold *Aspergillus* spp. concentrations of graphene and GO higher than 100 μg mL^{-1} are able to induce growth inhibition, apoptotic-like cell death responses and reduced production of extracellular enzymes.[25] At the molecular level, GO can compromise the structure and functioning of degradative enzymes such as lysozyme[26] and catalase.[27] Differently, GONRs or rGONRs and FLG flakes neither cause an impairment of LiP activity *in vitro*,[20] nor of LME activity *in vivo*,[13] respectively.

The present study has a two-fold aim: i) to investigate the fungal toxicity and biodegradability of GO in one-, two- and four-month old cultures of *P. chrysosporium*; and ii) to verify the *in vitro* degradation capabilities of two key LMEs secreted by *P. chrysosporium*, namely LiP against GO, FLG, and rGO, and Lac specifically targeting GO.

Materials and methods

Graphene oxide and graphene-related materials

GO was kindly supplied by Graphenea (San Sebastián, ES). It was characterized using a LECO CHNS-932 analyser (LECO Corporation, St. Joseph, MI, USA) to assess the content of C, H, N and S and an inVia Raman microscope (Renishaw, Wotton-under-Edge, GB) to acquire Raman spectra. Laser diffraction measurements along with high-resolution electron transmission microscopy (HR TEM JEOL 2100, by JEOL, Tokyo, JP) and environmental scanning electron microscopy (ESEM, Quanta™ 250 FEG, by FEI, Brno, CZ) were used to assess the lateral dimension and particle thickness of flakes.[71,72]

In this study rGO and FLG were also used to verify their degradability by LiP *in vitro*. rGO was provided by Graphenea and characterised like GO. FLG was prepared by ball milling treatment, starting from a mixture of graphite (7.5 mg of SP-1 graphite powder, Bay Carbon, US) and melamine (22.5 mg of 1,3,5-triazine-2,4,6-triamine, Sigma-Aldrich, DE).[28] The resulting solid mixture was suspended in water and melamine was washed away by dialyzing against water. In addition to the aforementioned analyses, FLG powder was characterized also by TGA.

Experiment 1: interactions between *P. chrysosporium* cultures and GO

An axenic strain (CBS 246.84) of *P. chrysosporium* was purchased from Westerdijk Fungal Biodiversity Institute (Utrecht, NL). The fungus was sub-cultured in Microbox Junior 40 vessels (Duchefa Biochemie, NL) filled with 20 g of solid malt extract agarose medium (MEG) composed of 30 g L^{-1} malt extract, 5 g L^{-1} peptone from meat, and 15 g L^{-1} agar. The fungus was grown at 18 μmol photons m^{-2} s^{-1} with a light/darkness cycle of 14/10 h at 20 °C until the development of abundant biomass.

After one month, fungal biomass was harvested, weighed, and fragmented with a tissue grinder in liquid MEG to prepare a fungal suspension of 50 mg mL^{-1}. A sterile 100 μg mL^{-1} GO suspension was prepared by dispersing the material in a suitable amount of MilliQ® water, sonicating it 6 times for 10 sec at 35 kHz (ref. 28) and pasteurizing it twice at 60 °C for 30 min. Then, 200 μL of fungal suspension were inoculated in 25 mL Erlenmeyer's flasks filled with 10 mL of MEG enriched with 0 (control cultures), 12.5, 25 or 50 μg mL^{-1} of GO (treated cultures) and allowed to grow in the dark at 20 °C for one (T_1), two (T_2), and four (T_4) months. Overall, 3 to 4 replicates were prepared for each GO concentration and incubation time. A further set of 25 mL Erlenmeyer's flasks containing non-inoculated liquid MEG enriched with 12.5, 25 and 50 μg mL^{-1} of GO (axenic controls) was prepared in triplicate to monitor the potential change of GO over time due to the compounds of the medium.

At the end of each incubation time (T_1–T_4), control and treated cultures were sonicated as before to detach the GO that potentially adhered to the internal surfaces of the Erlenmeyer's flasks. Then, the whole cultures, *i.e.*, the fungal biomass and the liquid medium, were transferred into polypropylene tubes and centrifuged at 6000 rpm for 3 min to pellet the fungus. The liquid medium was recovered, immediately frozen in liquid nitrogen and stored at −20 °C until biochemical analyses were conducted. The pelleted fungal biomass was transferred into pre-weighed and labelled Eppendorf vials, then frozen in liquid nitrogen, lyophilized for 48 h and weighed.

Liquid media of control and treated cultures were subjected to pH measurements and to three biochemical assays after thawing them at room temperature. Culture media pH was measured on 0.5 mL aliquots by means of a HI5521-02 pH-meter (Hanna Instruments, US) coupled to a microprobe with a sensitivity of ±0.002 (HI1083B, Hanna Instruments, US). Other 2.5 mL samples were filtered (0.2 μm) and processed to evaluate spectrophotometrically the content of H_2O_2 and the activity of lignin peroxidase (LiP) and laccase (Lac) in culture media according to Candotto Carniel *et al.* (2021).[13] The content of H_2O_2, or that of the reaction products of LiP and Lac assays (*i.e.*, veratryl aldehyde and the cation radical $ABTS^{\bullet+}$, respectively) was standardised per mg of lyophilised fungal biomass.

Experiment 2: assessing the effectiveness of the LiP catalytic cycle in degrading GRMs

A second experiment was carried out to test the interaction between LiP and three GRMs with a different oxygen/carbon ratio, namely FLG, GO and rGO. Suspensions of 100 μg mL^{-1} were prepared by dispersing a known amount of each GRM in a suitable volume of tartaric acid/sodium tartrate buffer solution (50 : 13 v/v; pH = 3) and sonicating the resulting suspension for 1 min. Lyophilised LiP powder was dispersed in tartrate buffer solution to a final concentration of 5 mg mL^{-1}. Then, LiP suspensions were vortexed for a few seconds and centrifuged at 2000*g* for 2 min to pellet and discharge the insoluble residuals. Aqueous solutions, 0.21 M ultra-pure H_2O_2 30% (Merk) and 1.5 M veratryl alcohol (VA; Sigma Aldrich), were used as LiP substrates.

The experiments were carried out according to a single factor design with four levels corresponding to the presence (+) and/or absence (−) of LiP and/or VA in experimental samples. Overall, four samples were prepared in glass vials containing 0.5 mL of FLG, GO or rGO suspension to which different amounts of buffer solutions, LiP suspension 150 μg mL^{-1}, and/or 1.5 M VA solution were added. Samples lacking both the enzyme and the substrate (*i.e.*, −LiP −VA) correspond to the experimental controls; those containing only 30 μL of LiP suspension (*i.e.*, +LiP −VA), 5.6 μL of veratryl alcohol (*i.e.*, −LiP +VA) or containing both compounds (*i.e.*, +LiP +VA) correspond to the experimental treatments. In the samples without the enzyme and/or the substrate, the amount of LiP and/or VA was substituted with an equal volume of buffer solution. The samples were brought to a volume of 996 μL with buffer solution and the LiP catalytic cycle was activated by adding 4 μL of 0.21 M H_2O_2 to control and treated samples (final volume of samples was 1 mL). The preliminary test showed that the initial amount of VA added to the buffer solution (in −LiP +VA and +LiP +VA samples) was sufficient to activate 5 enzymatic cycles (Fig. S1a†). Further aliquots were added maintaining the nominal concentration needed for the enzyme activation. On the contrary, the amount of H_2O_2 and LiP in +LiP −VA and +LiP +VA samples had to be renewed every 45 min at the end of each cycle (Fig. S1b†).

The long-term activation of the LiP catalytic cycle in +LiP +VA samples was maintained for 8 h for three days by adding increasing amounts of 0.21 M H_2O_2 and 150 μg mL^{-1} LiP every 45 min and 1.5 M VA every 225 min.

Experiment 3: assessing the effectiveness of Lac in degrading GO

To test if isolated Lac (Sigma Aldrich, Darmstadt, Germany) can degrade/modify GO under controlled conditions, a GO suspension of 50 μg mL^{-1} was prepared in acetate buffer (0.1 M; pH = 4.5, *i.e.* the optimal pH for Lac activity) and incubated with the enzyme. The experimental design tested the Lac-mediated GO degradation in the presence (+) and/or absence (−) of H_2O_2. Solutions of Lac and H_2O_2 at 1 U mL^{-1} and 1 mM, respectively, were prepared in acetate buffer. GO suspensions without Lac and H_2O_2 (*i.e.* −Lac −H_2O_2) were used as control samples. Samples incubated with Lac were composed of 250 μL of GO suspension, 40 μL of Lac plus 10 μL of buffer (*i.e.* +Lac −H_2O_2) or 10 μL of H_2O_2 (*i.e.* +Lac +H_2O_2). Both control and treated samples were prepared in triplicate and incubated for three days at 27 ± 1.5 °C under continuous orbital shaking.

TEM and Raman analyses

TEM observations and Raman analyses were used to assess the possible oxidation of GRMs due to the activity of *P. chrysosporium* enzymes in culture media or the LiP catalytic cycle activated *in vitro*. An aliquot of 7 μL of the treated and axenic culture liquid media of the first experiment (see section 2.2) and the control and treated samples of the second experiment were drop-cast onto pure carbon grids (3 mm, 200 mesh) and allowed to dry under controlled conditions (relative humidity <5%) for 48 h. The grids were observed with a TEM Philips EM208 (Philips, NL) operating at 100 kV and equipped with a Quemesa EMSIS camera (EMSIS, DE).

GO used in the first experiment was recovered and analysed as follows: for each replicate, a few milligrams of fungal biomass were excised, dispersed in 200 μL of MilliQ® water and sonicated for 5 min. Then, 60 μL were drop-cast onto polysine glass slides (Thermo-Scientific, US), allowed to dry as explained before and analysed with an inVia Raman

microscope (Renishaw, GB) at 532 nm with a 100× objective and an incident power of 1% (1 mW μm^{-2}).

Aliquots of 300 μL from control and treated samples of the second experiment were mixed with pure ethanol to remove the organic residuals adhered on GRM surfaces.[24] GRMs were then separated from the alcoholic solution by vacuum-filtration using a 0.025 μm mesh MF-Millipore filter-membrane (diameter 2.5 cm, Merck). GRMs were recovered by soaking the filter-membrane in 1 mL of MilliQ® water and sonicating it for 5 min. The membrane was discharged and 60 μL of the MilliQ® water were processed as explained before for Raman analysis.

GO samples from the third experiment exhibited deliquescent behaviour. To mitigate this, the samples were diluted 1 : 10 in MilliQ® water prior to analysis. Aliquots of 60 μL were then taken for Raman analysis, following the same procedure previously described.

Overall, 8 to 15 GRM flakes for each replicate of the three experiments were analysed with Raman, for a total of more than 400 measurements.

XPS and TGA analyses

The liquid media of three replicates of T_1 fungal cultures exposed to 50 μg mL^{-1} of GO were processed for recovering GO flakes, which were then analysed by XPS and TGA. Fungal cultures were mixed in a vial and centrifuged at 6000 rpm for 10 min. Because a major part of administered GO was retained by fungal biomass, the supernatant was removed and preserved while 10 mL of MilliQ® water was added to the pelleted fungus, which was subsequently vortexed, sonicated and centrifuged again. This separation process was repeated 8 times. Finally, the supernatants were mixed, vortexed and centrifuged at 6000 rpm. At the end, approximately 2.5 mg of GO were recovered, lyophilised and prepared for XPS and TGA analysis.

XPS measurements were performed in a SPECS system (Berlin, DE) equipped with a Phoibos 150 1D-DLD analyser and a 3 monochromatic Al Kα radiation sources (1486.7 eV). An initial analysis was carried out to analyse the corresponding elements (wide scan: step energy 1 eV, dwell time 0.1 s, pass energy 80 eV) and high resolution analysis was carried out (detail scan: step energy 0.08 eV, dwell time 0.1 s, pass energy 30 eV) with an electron exit angle of 90°. Fitting of the XPS data was done using CasaXPS 2.3.16 PR 1.6 software.

TGA measurements were performed with a TGA Q500 (TA Instruments) under N_2 atmosphere. The samples were introduced inside a platinum crucible and equilibrated at 100 °C followed by a 10 °C min^{-1} ramp between 100 and 800 °C.

Data analysis

The results of pH measurements and biochemical assays carried out on liquid media of fungal cultures were statistically analysed with two-way ANOVA using the GO concentration, the incubation time, and their interaction as categorical predictors. Raman spectra of GO treated with fungal cultures were elaborated in R environment to remove spikes and to correct the spectra baseline with polynomial baseline function and smoothing algorithms. The spectra were standardised within a 0–1 range and the intensity (I) of D and G bands as well as their ratio [$I_{(D)}/I_{(G)}$] was calculated and statistically analysed with two-way ANOVA as explained before.

The Raman spectra of the three GRMs treated with LiP or Lac in the second and third experiment, respectively, were pre-processed as explained before and statistically analysed with one-way ANOVA using the treatments (*i.e.* –LIP –VA, +LIP –VA, –LIP +VA and +LIP +VA or –Lac $-H_2O_2$, +Lac $+H_2O_2$, +Lac $-H_2O_2$) as categorical predictors.

Results

Characterization of GO and the other GRMs

The characterization of untreated GO and rGO was performed by Graphenea.[71,72] GO was supplied as a concentrated aqueous suspension (4 mg mL^{-1}) with a monolayer content >95% and an average particle size <10 μm. Elemental analysis indicated that GO is mostly composed of C (49–56%) and O (41–50%) with little amounts of N (<1%), H (<2%) and S (<3%) (Table S1†). The presence of N and S derives from the synthesis method, which is based on the oxidation of graphite using a mixture of nitric and sulphuric acid in the presence of $KMnO_4$. Regarding rGO powder, the particle size distribution measured by laser diffraction ranged from 1 to 15 μm. This material is mostly made of C (80–87%) and O (13–17%), while the content of N, S and H was found below 1% (Table S1†). The Raman spectra of GO and rGO show the two intense D and G bands at ~1345 and ~1580 cm^{-1}, respectively. Contrary to FLG, the $I_{(D)}/I_{(G)}$ ratios of both GO and rGO are ≈1.

The TGA performed on FLG confirmed the absence of carbonaceous impurities and functional groups and showed that FLG was composed of >95% C (Fig. S2†). The Raman spectrum is characterized by the intense G band appearing at ~1580 cm^{-1}, and two additional less intense peaks at ~1345 and ~2700 cm^{-1}, corresponding to D and 2D bands, respectively (Fig. S2†). The $I_{(D)}/I_{(G)}$ ratio is 0.46 confirming a low level of defects on the FLG lattice. TEM observation revealed that the lateral size of the FLG flakes varied from 100 to 1000 nm (Fig. S2†).

Interaction between *P. chrysosporium* cultures and GO

The first experiment with fungi was aimed at investigating (i) the potential toxic effects of GO on *P. chrysosporium*, and (ii) the capability of the fungus to degrade the tested material. When exposed to increasing GO concentrations, *P. chrysosporium* cultures showed interesting trends in terms of mycelial growth, culture media pH variation, enzyme activity, and H_2O_2 production over time (Fig. 1a–e). Mycelial biomass increased from T_1 to T_4, in both control and treated cultures (Fig. 1a). However, the biomass increase at the same incubation time was not equal under all experimental

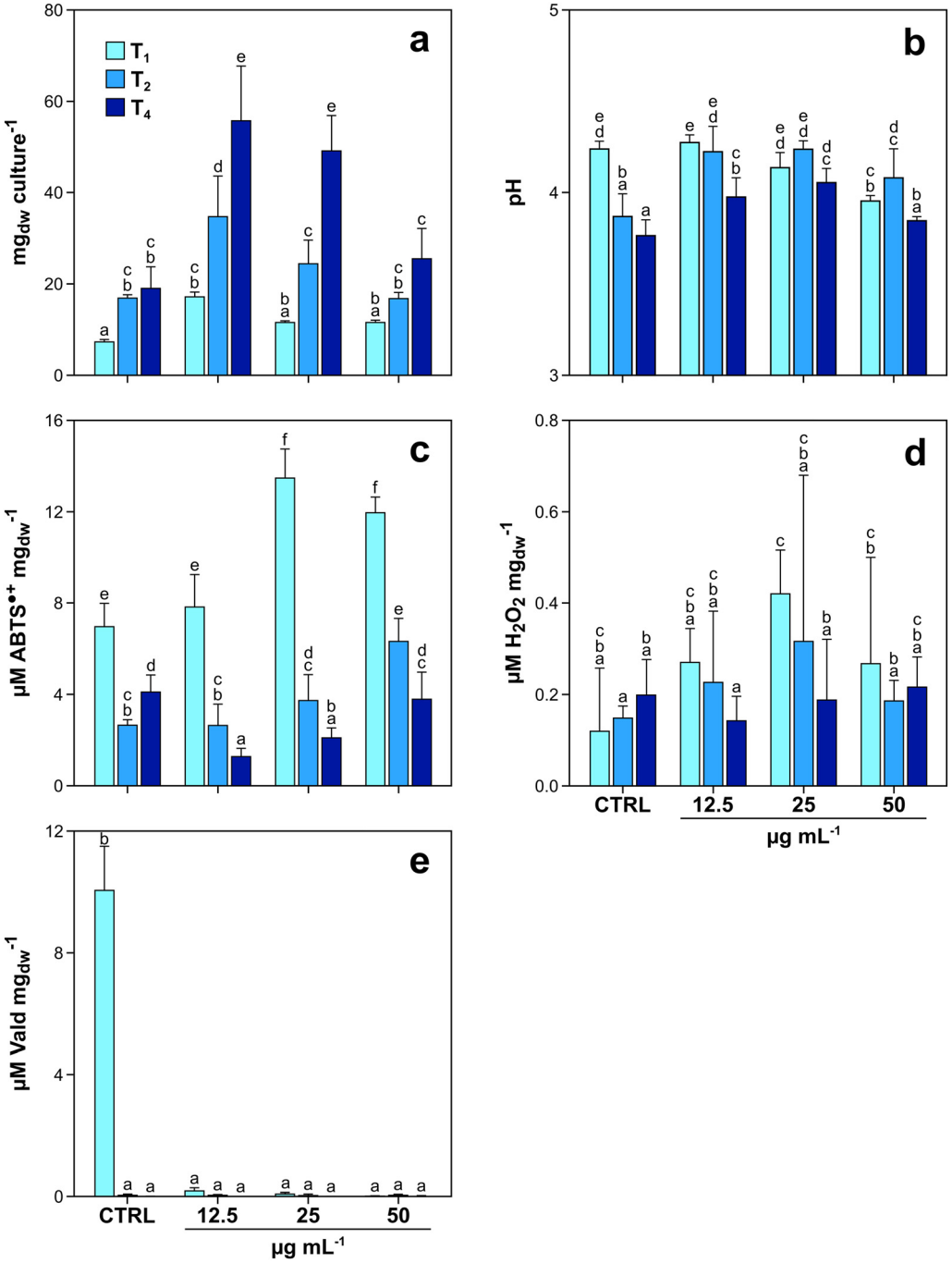

Fig. 1 Average values and standard deviation of mycelial biomass expressed as mg of fungal culture dry weight (mg_{dw}) (a), pH of culture medium (b), laccase activity (c), H_2O_2 content (d), and LiP activity (e), measured in *P. chrysosporium* cultures exposed to 0 (CTRL), 12.5, 25 and 50 μg mL^{-1} of GO for one (T_1), two (T_2) and four (T_4) months. Values are means ± s.d. (n = 4). Statistically different groups are marked with different letters (two-way ANOVA, LSD *post hoc* test).

conditions. T_1 control cultures grew 81.3, 45.5 and 45.3% less with respect to those treated with 12.5, 25 and 50 μg mL^{-1} of GO, respectively. The same trend was observed at T_2 and T_4 (Fig. 1a). The highest fungal growth with respect to the control was observed in T_4 cultures treated with the lowest GO concentration (+98%), while the biomass increase was progressively lower (88 and 28%, respectively) in those cultures exposed to 25 and 50 μg mL^{-1} of GO (Fig. 1a).

The measurements carried out on the media of control and treated cultures at T_1 indicated that increasing GO concentration in liquid media caused a pH decrease of 0.3 units (from 4.24 to 3.95) (Fig. 1b). Nevertheless, at T_2 and T_4, the pH variation trend changed, with the lowest values observed in the control cultures (3.77 at T_4). The biochemical analyses using ABTS as a substrate highlighted that the activity of laccase was not constant over time and increased

according to GO concentration (Fig. 1c) at T_1 and T_2. Interestingly, the same trend was observed for the content of H_2O_2 (Fig. 1d).

The assay on LiP activity provided positive results only in control cultures at T_1, while in older control cultures (T_2 and T_4) and in all treated ones (T_1–T_4), LiP activity was essentially absent with values below the limit of detection of the instrument, independent of GO concentrations (Fig. 1e).

TEM observations and Raman analyses carried out on GO samples exposed to fungal cultures clearly indicated an oxidation of the tested material (Fig. 2 and 3). The morphology of flakes recovered from axenic culture media differed from those exposed to fungal cultures. At T_1, the margins of GO flakes exposed to fungal cultures were rounded and folded (Fig. 2a–c). At T_4, holes started to appear on the surface of flakes (Fig. 2f, g and k). In addition, the surface of most of the flakes had peculiar, circular structures, whose margins showed an enhanced Moiré effect (Fig. 2a). These signs were independent of the tested concentration and/or incubation time. Accordingly, the Raman spectra of GO recovered from *P. chrysosporium* cultures at T_1 had an average $I_{(D)}/I_{(G)}$ value 16.1 and 12.3% higher than that observed for spectra of untreated GO flakes and those recovered from axenic, non-inoculated medium at T_4, respectively (Fig. 3 and S3†). However, significant differences among the $I_{(D)}/I_{(G)}$ ratio of the GO flakes sampled from cultures treated with different concentrations (12.5–50 μg mL^{-1}) for the selected incubation time were not observed.

With the aim to corroborate the increase of the oxidation degree of GO observed at T_1, XPS and TGA analysis were performed at a GO concentration of 50 μg mL^{-1} (Fig. S4†). Regarding XPS, when we compare the C1s and O1s peaks of the pristine GO and the material recovered after one month of incubation (Fig. S4a and b†) it was very challenging to discriminate the contribution of the biological matrix from that of the bare material, due to their organic nature. Not surprisingly, the C/O atomic ratio increased along with nitrogen content (Table S2†), indicating the presence of residues from

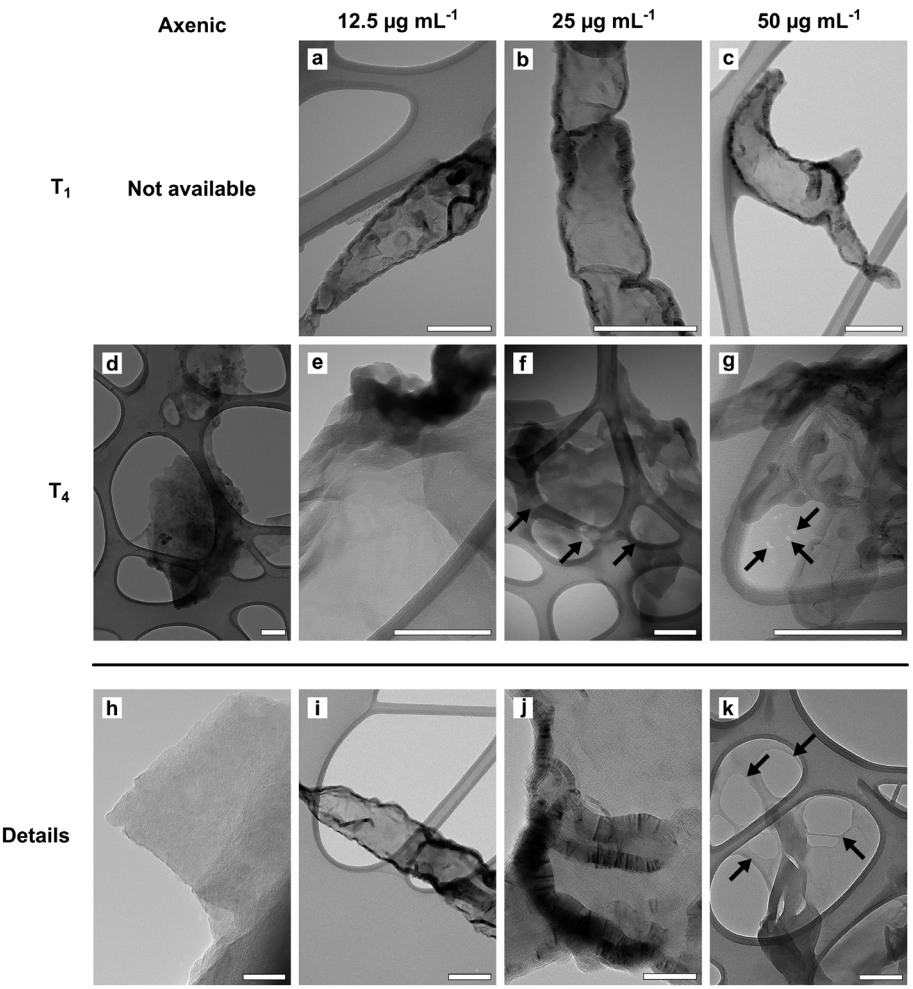

Fig. 2 TEM micrographs of GO flakes incubated in axenic culture media (d) or in *P. chrysosporium* cultures (a–c and e–g) for one (T_1; a–c) and four (T_4; d–g) months, at increasing GO concentrations: 12.5 (a and e), 25 (b and f), and 50 (c–g) μg mL^{-1}. Details of GO flakes (h–k): margins of flakes from axenic media (h) and from cultures of *P. chrysosporium* (i); Moirè effect by overlapping graphene layers (j); holes in the graphene lattice (k). Arrows: holes in the graphene lattice. Scale bars: a–i, *k* = 200 nm; *j* = 50 nm.

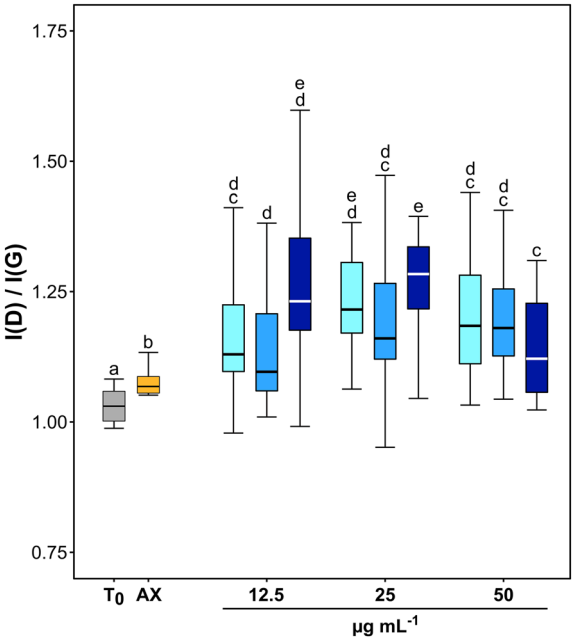

Fig. 3 Average and standard deviation of $I_{(D)}/I_{(G)}$ values calculated from Raman spectra acquired for untreated GO (T_0; grey boxplot), GO recovered from axenic culture media after four months (AX; orange boxplot) and from one, two- and four-month old *P. chrysosporium* cultures (light to dark blue boxplots, respectively) exposed to the three test concentrations: 12.5, 25 and 50 μg mL^{-1} of GO. Values are means ± s.d. (n = 6–25). Statistically different groups are marked with different letters (two-way ANOVA, Tukey's HSD *post hoc* test).

the cultivation process. TGA showed an increase in the weight loss of the material recovered after 1 month of incubation, which could be due to an increase in oxygen content. However, the maximum of the first derivative curve (Fig. S4c†) does not match with the maximum of the pristine GO, which was expected to increase together with an increase in oxygen content,[29] suggesting the presence of other species (again, residues from the cultivation process) on the surface of the incubated material, thus supporting the XPS results. TGA did not corroborate the increase in the degree of oxidation because the new maximum (~277 °C) masked the one associated with the presence of oxygenated groups (~187 °C).

Assessment of the efficiency of the LiP catalytic cycle in degrading GRMs

In order to verify the effectiveness of LiP in terms of GO degradation, questioned by the results reported above, the reaction products of the LiP catalytic cycle were tested in buffered aqueous suspensions using an experimental design, which also allowed the individual contribution of LiP and its substrates (*i.e.* H_2O_2 and VA) in the *in vitro* degradative process to be evaluated. The observations were extended to FLG and rGO. The experiment lasted for three days during which the LiP catalytic cycle was activated 31 times renewing at each cycle the content of enzyme and/or that of H_2O_2 and VA. Before activating each cycle, the activity of LiP was tested in turn in control samples non-containing GRMs by assessing the formation of veratraldehyde (VAld). Without GRMs, VAld concentration was 0.18 ± 0.06 mM (n = 13). At the end of the three days, the VAld concentration in the experimental samples containing the enzyme and the substrates (*i.e.* +LiP +VA samples) reached 0.14 mM, while in those deprived of the enzyme (*i.e.* −LiP +VA samples) the VAld concentration was 0.06 mM. These results indicate that the LiP catalytic cycle was activated but the enzymatic reaction was largely suppressed, possibly by the presence of GRMs.

TEM observations on GO showed that GO flakes had folded margins and wrinkled surfaces, without revealing significant differences among samples (Fig. 4b, e, h and k). Also, Raman analyses showed no evidence of degradation such as changes in the ratio between the bands D and G of treated samples with respect to control and untreated samples (Fig. 5b).

FLG flakes tended to form clusters composed of a few flakes each, which preserved well-defined, polygonal edges without showing signs of degradation on the lattice such as holes or rounded margins (Fig. 4a, d, g and j). Accordingly, the results of Raman analyses showed that the intensity of the FLG characteristic D and G bands or their ratio was similar in control and treated samples, thus excluding any physicochemical alteration due to the treatments (Fig. 5a). The only noteworthy difference concerns the presence of several punctiform structures on the flake surface recovered from +LiP −VA samples (Fig. 4g).

TEM images of rGO control samples evidenced that the flakes were very similar to those of FLG, but their surface was perforated by several holes (Fig. 4c, f, i and l). In this case the experimental treatments did not cause any morphological or Raman detectable change with respect to the control samples (Fig. 5c).

Assessment of the efficiency of laccase in degrading GO

In the third experiment, GO was treated with Lac in the presence and absence of H_2O_2 for three days. Laccase and H_2O_2 were added to GO samples, *i.e.* +Lac −H_2O_2 and +Lac +H_2O_2, at the beginning of the treatments, without performing further additions during the ongoing of the experiment as in the case of LiP. Raman analysis revealed that the $I_{(D)}/I_{(G)}$ ratio of GO from +Lac −H_2O_2 samples increased significantly with respect to control samples (~4%; Fig. 5d). Although it may seem a small difference, this value represents 25% of the average increase of the $I_{(D)}/I_{(G)}$ ratio observed in GO flakes incubated with *P. chrysosporium* for four months. On the contrary, Raman analysis on GO flakes from +Lac +H_2O_2 samples did not show any significant changes with respect to control samples (*i.e.* −Lac −H_2O_2; Fig. 5d).

Discussion

Effect of GO on fungal growth

Among GRMs, GO is particularly reactive and is relatively more toxic than FLG and rGO towards a wide range of

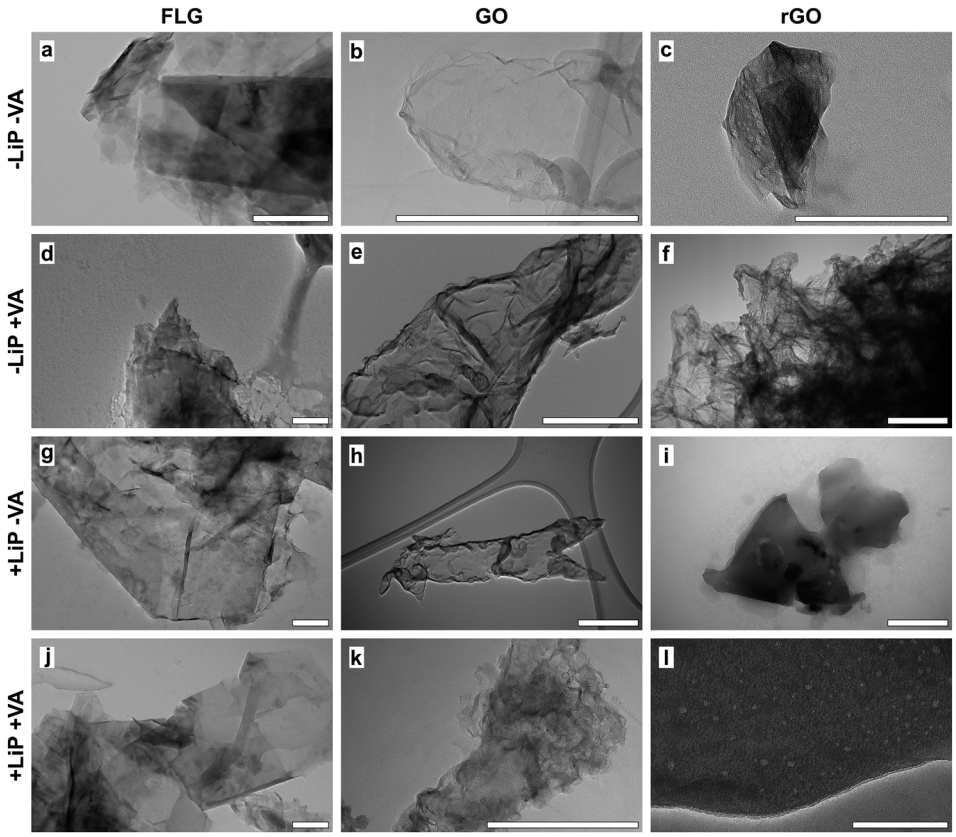

Fig. 4 TEM micrographs of FLG (first column, a–j), GO (second column, b–k) and rGO (third column, c–l) recovered after three days from tartaric acid/sodium tartrate buffer solution, in the presence (+, g–l) or absence (–, a–f) of LiP and/or its secondary substrate, VA (+VA, d–f; –VA, a–c) . Scale bars = 250 nm.

organisms, spanning from fungi[30] to plants[31–33] and animals.[34] This has been attributed to its inherent reactivity due to numerous oxygenated functional groups on its surface,[35] which also determine the intrinsic acidity. In fact, we found that after one month of incubation (T_1) with the mycelium, the pH of the liquid media was progressively lower with the increase of GO concentration compared to the pH of CTRL medium (Fig. 1b). However, in the case of fungi, this effect can be neglected, because these organisms thrive under acidic conditions, and the activity of their degradative enzymes finds its optimum at low pH.[36] Moreover, GO did not inhibit the development of *P. chrysosporium*; instead, it stimulated fungal growth at low GO concentrations (Fig. 1a). A similar "growth-stimulating effect" on fungi has been already described in other studies on GO and rGO.[24,30] The origin of this phenomenon has been attributed to hormesis, *i.e.*, growth stimulation by low doses of xenobiotics or other stressors,[37] which has rarely been documented.

White-rot fungi are chemo-organotrophic organisms and gain energy by oxidation of polymeric organic compounds (*e.g.* lignin) to a state of phenolic subunits and CO_2.[19] Phenolic compounds in low concentrations stimulate fungal growth and biosynthesis of ligninolytic enzymes,[38] but above a certain threshold, the same compounds become toxic and inhibit fungal growth through the formation of oxygen radicals.[39,40] The GO structure resembles that of a polymeric phenolic compound.[41] Therefore, its oxidation (*vide infra*) could produce lignin-like degradation by-products with similar toxicity to the fungus. An accumulation of phenolic compounds derived from progressive GO degradation would explain why, for the same incubation time, the higher the initial GO concentration in liquid media, the lower the "growth-stimulating effect".

This hypothesis is supported by the fact that *P. chrysosporium* produces 15 different laccase isoforms,[42] whose transcription is stimulated by the concentration of lignin degradation by-products,[43] and one of the functions of laccase is to oxidize and polymerize phenolic compounds to inactivate their toxicity.[39] During the degradation of polysaccharide and lignin, fungal laccase activity is strictly coordinated in a multi-enzymatic system, which depends on H_2O_2 production mediated by other enzymes (*e.g.* aryl alcohol oxidase and glyoxal oxidase).[44] At T_1, fungal cultures exposed to 25 and 50 μg mL^{-1} of GO grew equally with respect to control cultures and cultures exposed to 12.5 μg mL^{-1} of GO, but had higher laccase activity and higher H_2O_2 content (Fig. 1c and d).

Degradation of GO by *P. chrysosporium*

TEM observations and statistical analysis of Raman data clearly confirmed that the morphology and lattice of the GO

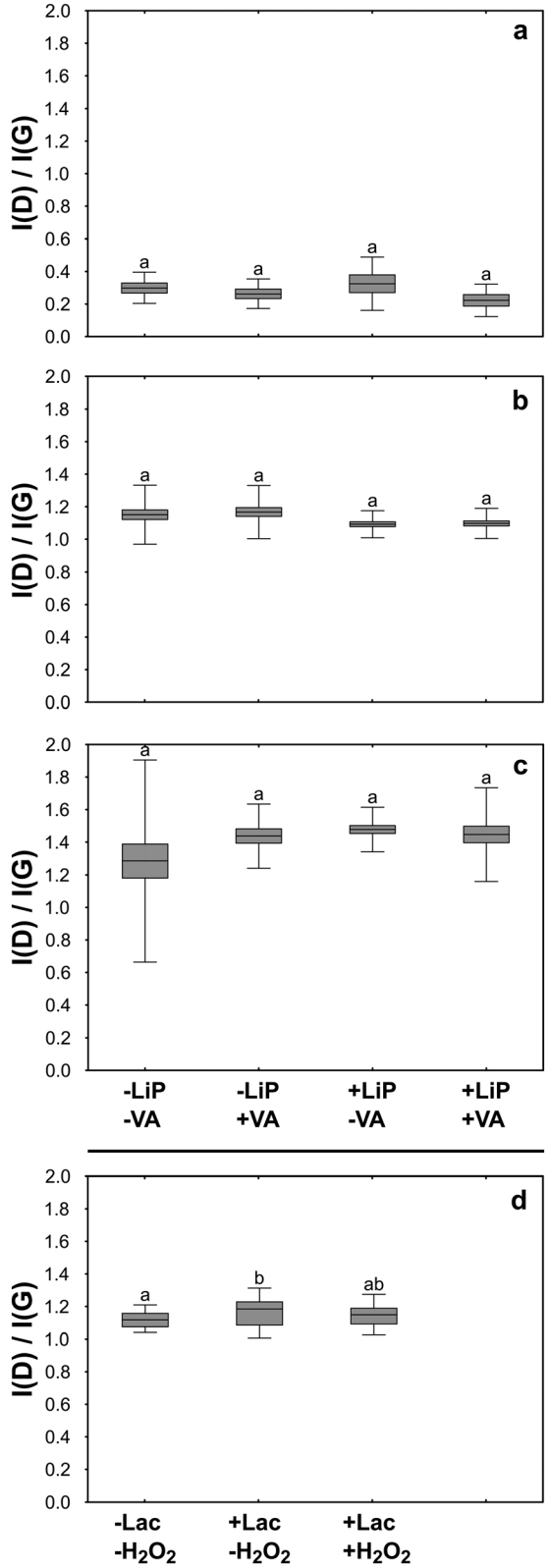

Fig. 5 Boxplots of the ratio between the intensity (I) of the D and G bands measured on FLG (a), GO (b) and rGO (c) flakes incubated for three days with (+) or without (–) LiP and/or its secondary substratum, VA. The last graph (d) reports the $I_{(D)}/I_{(G)}$ values measured on GO flakes incubated with Lac in the presence (+) or absence (–) of H_2O_2. Boxplots marked with different letters indicate statistically significant differences among groups of the same experiment as identified with ANOVA followed by Tukey's *post hoc* test.

flakes exposed to the *P. chrysosporium* cultures were significantly altered (Fig. 2 and 3). Some GO flakes showed an enhanced Moiré effect (Fig. 2j) indicating that more monolayers were superimposed, or the same flake had folded on itself.[45,46] However, most of them had rounded and wrinkled edges and holes (Fig. 2a–c, g and k), *i.e.*, all peculiar structures reported for other GRMs were successfully deteriorated *in vitro* by isolated enzymes or *in vivo* by other fungi.[13,21,46,47]

Statistical comparison of Raman spectra clearly showed that GO flakes exposed to *P. chrysosporium* cultures presented an increase in the $I_{(D)}/I_{(G)}$ ratio (Fig. 3). The intensity of the D band is commonly used as an indicator of the disorder of the crystal lattice of degraded GRMs.[48,49] Interestingly, the average values of the $I_{(D)}/I_{(G)}$ ratio after four months (T_4) increased with the decrease of GO concentration and with the increase of fungal biomass.

Unfortunately, XPS analysis could not validate the Raman results, because the GO flakes recovered from the fungal cultures had increased content of N and C, which made it impossible to compare the C/O ratio between pristine and treated GO flakes (Table S2†). However, these results indirectly confirm that GO flakes are particularly reactive in adsorbing N- and C-rich molecules, most likely chitin (an essential component of the fungal cell wall) and enzymes secreted into the medium (see below).

Interaction between GRMs and LiP

The monomeric glycosylated enzyme LiP catalyses the oxidation of veratryl alcohol to the veratryl alcohol cation radical, which is the intermediate reaction by-product responsible for the cleavage of aromatic rings, C_α–C_β bonds, and the oxidation of aromatic C_α in lignin as well as in other organic molecules.[50,51] Under these premises, LiP was considered the best candidate for the degradation of GO and other GRMs. However, the results of our experiments on the GO/*P. chrysosporium* interplay showed a lack of LiP activity at all three exposure times (T_1–T_4) (Fig. 1e). Since the culture media were not replenished between the incubation periods (to limit contamination and to force the fungus to degrade GO while peptides and sugars were consumed in the liquid media), the progressive decline in nutrient availability from month one (T_1) to month four (T_4) may have reduced LiP production.[52,53] However, after T_1 LiP activity was high in the control cultures and minimal where GO was present, as if the enzyme had been inactivated (Fig. 1e). To verify this result in an environment less complex than that created by a cultured fungus in its medium, we performed *in vitro* activation of a commercial *P. chrysosporium* LiP in the presence of GO, FLG and rGO. This experiment also confirmed the almost complete inactivation of the enzyme by all three GRMs, with no degradation observed (Fig. 5a–c). Conversely, Lalwani and coauthors,[46] who studied the *in vitro* degradation of GONRs and rGONRs by LiP, reported no impairment of LiP activity by the materials. This apparent contradiction can be

explained by differences in the interaction between the degrading enzyme(s) and the substrate. Notoriously, GRMs can spontaneously adsorb and immobilize proteins and other large molecules directly on their surface.[54,55] However, adsorbed enzymes do not always retain their tertiary structure, with possible impairment of their activity.[56,57] Adsorption is caused by electrostatic interactions, that depend, largely but not exclusively, on the electric charge density, the molecular mass of the molecules involved, and the ionic strength of the medium.[58] From this point of view, the structural and dimensional differences between the GONRs and rGONRs studied by Lalwani and coauthors[46] and the GRMs studied here could be sufficient to explain the different degradation ability of LiP towards nanoribbons and flakes.

Other factors need to be considered to explain the different behaviour of LiP and laccase in the presence of GRMs. The pH of the treated cultures of Fig. 1 ranged from 3.7 to 4.3, whereas the *in vitro* experiment of Fig. 5 was performed at pH 3. Under these conditions, LiP exhibits a slight positive charge due to the variation of isoelectric points (IP) among its isoforms, ranging from 3.70 to 4.65.[59] In contrast, laccase displays a negative charge, akin to GO, since the former presents an IP of less than 3.55,[60] whereas the latter has an IP of ~1.7.[61] In addition, the molecular mass of LiP (40 kDa)[59] is about half that of laccase (60–80 kDa),[39] therefore, LiP is more sensitive to the electrostatic attraction of GO than Lac.[62] TEM micrographs acquired for FLG, GO and rGO flakes seem to confirm a possible immobilization of LiP chains on their surface. Globular structures whose dimensions are fully compatible with LiP were frequently observed on the GRM flake surfaces of +LiP −VA samples (Fig. 4g). Similar structures were described by Zhang *et al.* (2010)[54] and Kishore *et al.* (2012)[63] in studies specifically addressing the immobilisation of enzymes onto the GRM lattices. Further experimental work may confirm this conclusion.

The role of Lac in GO degradation

Cultures *of P. chrysosporium* degraded GO despite this material significantly interfering with the catalytic cycle of LiP both in culture (first experiment) and under *in vitro* conditions (second experiment; see previous sections). These unexpected findings laid the groundwork to set the third experiment, which led to the observation that Lac activity increased the $I_{(D)}/I_{(G)}$ ratio of GO after an incubation period of three days only (Fig. 5d). This evidence supports the hypothesis that the GO degradation mediated by *P. chrysosporium* cultures could be primarily attributed to the activity of Lac rather than LiP (Fig. 5).

Interestingly, to the best of our knowledge, the present study is the first to provide evidence of Lac-mediated degradation of GO, although this enzyme has been successfully used in several studies focused on the degradation of dyes,[64] biocides,[65] as well as on the delignification of organic matter.[66] Different from LiP and other lignolytic enzymes, Lac oxidizes carbon-based substrata also without a mediator molecule.[67] The resulting degradative processes are thus based on a direct electron transfer from a substrate (*e.g.* GO in our case) to an oxidant, typically molecular oxygen, producing water and reactive oxygen species (ROS), including H_2O_2 as by-products.[68] However, it is known that the proper functioning of Lac can be influenced by the concentration of H_2O_2 in the reaction media. On the one hand, H_2O_2 may enhance the oxidation of certain substrates by providing an additional source of oxygen. On the other hand, it can lead to the generation of other ROS that might interfere with the reaction or affect the stability of laccase itself.[69] This peculiar relationship between Laccase and H_2O_2 is in full agreement with our results. Laccase activity and H_2O_2 concentration in fungal cultures had similar trends (Fig. 1c and d), meaning that *P. chrysosporium* finely controlled the multi-enzymatic degradative apparatus in the liquid media. In the third experiment, instead, the addition of H_2O_2 in +Lac +H_2O_2 samples, which represents a not metabolically controlled system, likely interfered with Lac activity and thus prevented GO degradation (Fig. 5d).

Conclusions and environmental relevance

The presence of GO flakes in liquid media is fully compatible with the development of *P. chrysosporium* cultures to the extent that it is able to stimulate fungal growth in inverse proportion to its concentration. Surprisingly, the degradation process of GO is not mediated by LiP but by Lac isoforms. These results are particularly important because they indicate that Lac isoforms may play a fundamental role in the degradation of GO in the environment. Laccases are ubiquitous oxidative enzymes found in all biological kingdoms,[70] not restricted, like LiP, to an ecologically highly specialised group of fungi. Therefore, it is plausible to assume that GO-based materials released unintentionally or voluntarily into terrestrial ecosystems will be (slowly) degraded by a range of laccase-bearing/releasing organisms.

Author contributions

Lorenzo Fortuna: data curation, formal analysis, investigation, methodology, visualization, writing original draft; Marina Garrido: investigation, methodology, writing original draft; Davide Zanelli: investigation, methodology; Humberto Castillo Gonzalez: investigation, methodology; Cristina Martín: methodology; Fabio Candotto Carniel: conceptualization, data curation, investigation, methodology, visualization, writing - original draft, writing – review & editing; Ester Vázquez: conceptualization, resources, supervision, writing – review & editing; Maurizio Prato: conceptualization, funding acquisition, project administration, supervision; Alberto Bianco: conceptualization, funding acquisition, resources, supervision, writing – review & editing; Mauro Tretiach: conceptualization,

project administration, resources, supervision; writing – review & editing.

Conflicts of interest

There are no conflicts to declare.

Acknowledgements

This work was supported by the Graphene Flagship Core 2 and 3 grant agreement (no. 785219 and 881603), which covered the activity of Dr. Lorenzo Fortuna, Dr. Marina Garrido, and Dr. Fabio Candotto Carniel. The activity of Dr. Davide Zanelli was covered by the doctoral scholarship "DOTTAMBIENTEVITA34-18" of the University of Trieste. This work was partly supported by the Agence Nationale de la Recherche (ANR) through the LabEx project Chemistry of Complex Systems (ANR-10-LABX-0026_CSC) and by the Spanish Ministerio de Ciencia e Innovación (Project PDC2021-120735-I00). We wish to acknowledge the Centre National de la Recherche Scientifique (CNRS) and the International Center for Frontier Research in Chemistry (icFRC). The authors thank Dr. Alejandro Criado (Universidade da Coruña, Centro de Investigacións Científicas Avanzadas) for XPS analyses.

References

1 D. Akinwande, C. J. Brennan, J. S. Bunch, P. Egberts, J. R. Felts, H. Gao, R. Huang, J.-S. Kim, T. Li, Y. Li, K. M. Liechti, N. Lu, H. S. Park, E. J. Reed, P. Wang, B. I. Yakobson, T. Zhang, Y.-W. Zhang, Y. Zhou and Y. Zhu, A review on mechanics and mechanical properties of 2D materials—Graphene and beyond, *Extreme Mech. Lett.*, 2017, **13**, 42–77.

2 A. C. Ferrari, F. Bonaccorso, V. Fal'ko, K. S. Novoselov, S. Roche, P. Bøggild, S. Borini, F. H. L. Koppens, V. Palermo, N. Pugno, J. A. Garrido, R. Sordan, A. Bianco, L. Ballerini, M. Prato, E. Lidorikis, J. Kivioja, C. Marinelli, T. Ryhänen, A. Morpurgo, J. N. Coleman, V. Nicolosi, L. Colombo, A. Fert, M. Garcia-Hernandez, A. Bachtold, G. F. Schneider, F. Guinea, C. Dekker, M. Barbone, Z. Sun, C. Galiotis, A. N. Grigorenko, G. Konstantatos, A. Kis, M. Katsnelson, L. Vandersypen, A. Loiseau, V. Morandi, D. Neumaier, E. Treossi, V. Pellegrini, M. Polini, A. Tredicucci, G. M. Williams, B. Hee Hong, J.-H. Ahn, J. Min Kim, H. Zirath, B. J. van Wees, H. van der Zant, L. Occhipinti, A. Di Matteo, I. A. Kinloch, T. Seyller, E. Quesnel, X. Feng, K. Teo, N. Rupesinghe, P. Hakonen, S. R. T. Neil, Q. Tannock, T. Löfwander and J. Kinaret, Science and technology roadmap for graphene, related two-dimensional crystals, and hybrid systems, *Nanoscale*, 2015, **7**, 4598–4810.

3 K. S. Novoselov, A. K. Geim, S. V. Morozov, D. Jiang, Y. Zhang, S. V. Dubonos, I. V. Grigorieva and A. A. Firsov, Electric field effect in atomically thin carbon Films, *Science*, 2004, **306**, 666–669.

4 M. Cai, D. Thorpe, D. H. Adamson and H. C. Schniepp, Methods of graphite exfoliation, *J. Mater. Chem.*, 2012, **22**, 24992.

5 A. T. Dideikin and A. Y. Vul', Graphene oxide and derivatives: the place in graphene family, *Front. Phys.*, 2019, **6**, 149.

6 S. Abdolhosseinzadeh, H. Asgharzadeh and H. Seop Kim, Fast and fully-scalable synthesis of reduced graphene oxide, *Sci. Rep.*, 2015, **5**, 10160.

7 H. Yang, X. Wu, Q. Ma, A. Yilihamu, S. Yang, Q. Zhang, S. Feng and S.-T. Yang, Fungal transformation of graphene by white rot fungus *Phanerochaete chrysosporium*, *Chemosphere*, 2019, **216**, 9–18.

8 W. K. Chee, H. N. Lim, N. M. Huang and I. Harrison, Nanocomposites of graphene/polymers: a review, *RSC Adv.*, 2015, **5**, 68014–68051.

9 C. Liu, X. Huang, Y. Y. Wu, X. Deng, J. Liu, Z. Zheng and D. Hui, Review on the research progress of cement-based and geopolymer materials modified by graphene and graphene oxide, *Nanotechnol. Rev.*, 2020, **9**, 155–169.

10 X. Wang, H. Xie, Z. Wang and K. He, Graphene oxide as a pesticide delivery vector for enhancing acaricidal activity against spider mites, *Colloids Surf., B*, 2019, **173**, 632–638.

11 S. Kabiri, F. Degryse, D. N. H. Tran, R. C. da Silva, M. J. McLaughlin and D. Losic, Graphene Oxide: a new carrier for slow release of plant micronutrients, *ACS Appl. Mater. Interfaces*, 2017, **9**, 43325–43335.

12 Y. Qu, J. Wang, Q. Ma, W. Shen, X. Pei, S. You, Q. Yin and X. Li, A novel environmental fate of graphene oxide: Biodegradation by a bacterium Labrys sp. WJW to support growth, *Water Res.*, 2018, **143**, 260–269.

13 F. Candotto Carniel, L. Fortuna, D. Zanelli, M. Garrido, E. Vázquez, V. J. González, M. Prato and M. Tretiach, Graphene environmental biodegradation: Wood degrading and saprotrophic fungi oxidize few-layer graphene, *J. Hazard. Mater.*, 2021, **414**, 125553.

14 E. M. Ostrem Loss and J. H. Yu, Bioremediation and microbial metabolism of benzo(a)pyrene, *Mol. Microbiol.*, 2018, **109**, 433–444.

15 A. K. Singh, M. Bilal, H. M. N. Iqbal, A. S. Meyer and A. Raj, Bioremediation of lignin derivatives and phenolics in wastewater with lignin modifying enzymes: Status, opportunities and challenges, *Sci. Total Environ.*, 2021, **777**, 145988.

16 T. K. Lundell, M. R. Mäkelä and K. Hildén, Lignin-modifying enzymes in filamentous basidiomycetes - ecological, functional and phylogenetic review, *J. Basic Microbiol.*, 2010, **50**, 5–20.

17 M. Čvančarová, Z. Křesinová, A. Filipová, S. Covino and T. Cajthaml, Biodegradation of PCBs by ligninolytic fungi and characterization of the degradation products, *Chemosphere*, 2012, **88**, 1317–1323.

18 T. Kadri, T. Rouissi, S. Kaur Brar, M. Cledon, S. Sarma and M. Verma, Biodegradation of polycyclic aromatic hydrocarbons (PAHs) by fungal enzymes: A review, *J. Environ. Sci.*, 2017, **51**, 52–74.

19 M. E. Brown and M. C. Chang, Exploring bacterial lignin degradation, *Curr. Opin. Chem. Biol.*, 2014, **19**, 1–7.

20 G. Lalwani, W. Xing and B. Sitharaman, Enzymatic degradation of oxidized and reduced graphene nanoribbons by lignin peroxidase, *J. Mater. Chem. B*, 2014, **2**, 6354–6362.

21 R. Kurapati, J. Russier, M. A. Squillaci, E. Treossi, C. Ménard-Moyon, A. E. Del Rio-Castillo, E. Vazquez, P. Samorì, V. Palermo and A. Bianco, Dispersibility-dependent biodegradation of graphene oxide by myeloperoxidase, *Small*, 2015, **11**, 3985–3994.

22 R. Kurapati, S. P. Mukherjee, C. Martín, G. Bepete, E. Vázquez, A. Pénicaud, B. Fadeel and A. Bianco, Degradation of single-layer and few-layer graphene by neutrophil myeloperoxidase, *Angew. Chem., Int. Ed.*, 2018, **57**, 11722–11727.

23 B. Fadeel, C. Bussy, S. Merino, E. Vázquez, E. Flahaut, F. Mouchet, L. Evariste, L. Gauthier, A. J. Koivisto, U. Vogel, C. Martín, L. G. Delogu, T. Buerki-Thurnherr, P. Wick, D. Beloin-Saint-Pierre, R. Hischier, M. Pelin, F. Candotto Carniel, M. Tretiach, F. Cesca, F. Benfenati, D. Scaini, L. Ballerini, K. Kostarelos, M. Prato and A. Bianco, Safety assessment of graphene-based materials: focus on human health and the environment, *ACS Nano*, 2018, **12**, 10582–10620.

24 H. Yang, S. Feng, Q. Ma, Z. Ming, Y. Bai, L. Chen and S.-T. Yang, Influence of reduced graphene oxide on the growth, structure and decomposition activity of white-rot fungus Phanerochaete chrysosporium, *RSC Adv.*, 2018, **8**, 5026–5033.

25 H. N. Nguyen, C. Chaves-Lopez, R. C. Oliveira, A. Paparella and D. F. Rodrigues, Cellular and metabolic approaches to investigate the effects of graphene and graphene oxide in the fungi *Aspergillus flavus* and *Aspergillus niger*, *Carbon*, 2019, **143**, 419–429.

26 Y. Bai, Z. Ming, Y. Cao, S. Feng, H. Yang, L. Chen and S.-T. Yang, Influence of graphene oxide and reduced graphene oxide on the activity and conformation of lysozyme, *Colloids Surf., B*, 2017, **154**, 96–103.

27 X.-L. Wei and Z.-Q. Ge, Effect of graphene oxide on conformation and activity of catalase, *Carbon*, 2013, **60**, 401–409.

28 J. M. Gonzáles-Domínguez, V. León, M. I. Lucío, M. Prato and E. Vázquez, Production of ready-to-use few-layer graphene in aqueous suspensions, *Nat. Protoc.*, 2018, **13**, 495–506.

29 F. Farivar, P. L. Yap, K. Hassan, T. T. Tung, D. N. H. Tran, A. J. Pollard and D. Losic, Unlocking thermogravimetric analysis (TGA) in the fight against "Fake graphene" materials, *Carbon*, 2021, **179**, 505–513.

30 J. Xie, Z. Ming, H. Li, H. Yang, B. Yu, R. Wu, X. Liu, Y. Bai and S. T. Yang, Toxicity of graphene oxide to white rot fungus *Phanerochaete chrysosporium*, *Chemosphere*, 2016, **151**, 324–331.

31 F. Candotto Carniel, L. Fortuna, M. Nepi, G. Cai, C. Del Casino, G. Adami, M. Bramini, S. Bosi, E. Flahaut, C. Martín, E. Vázquez, M. Prato and M. Tretiach, Beyond graphene oxide acidity: Novel insights into graphene related materials effects on the sexual reproduction of seed plants, *J. Hazard. Mater.*, 2020, **393**, 122380.

32 D. Zanelli, F. C. Carniel, L. Fortuna, E. Pavoni, V. J. González, E. Vázquez, M. Prato and M. Tretiach, Is airborne graphene oxide a possible hazard for the sexual reproduction of wind-pollinated plants?, *Sci. Total Environ.*, 2022, **830**, 154625.

33 D. Zanelli, F. Candotto Carniel, L. Fortuna, E. Pavoni, V. Jehová González, E. Vázquez, M. Prato and M. Tretiach, Interactions of airborne graphene oxides with the sexual reproduction of a model plant: When production impurities matter, *Chemosphere*, 2023, **312**, 137138.

34 M. Ema, M. Gamo and K. Honda, A review of toxicity studies on graphene-based nanomaterials in laboratory animals, *Regul. Toxicol. Pharmacol.*, 2017, **85**, 7–24.

35 A. M. Dimiev, L. B. Alemany and J. M. Tour, Graphene oxide. Origin of acidity, its instability in water, and a new dynamic structural model, *ACS Nano*, 2013, **7**, 576–588.

36 O. A. Kudryavtseva, Y. E. Dunaevsky, O. V. Kamzolkina and M. A. Belozersky, Fungal proteolytic enzymes: Features of the extracellular proteases of xylotrophic basidiomycetes, *Microbiology*, 2008, **77**, 643–653.

37 A. R. D. Stebbing, Hormesis — The stimulation of growth by low levels of inhibitors, *Sci. Total Environ.*, 1982, **22**, 213–234.

38 T. Robinson and P. S. Nigam, Remediation of textile dye waste water using a white-rot fungus Bjerkandera adusta through solid-state fermentation (SSF), *Appl. Biochem. Biotechnol.*, 2008, **151**, 618–628.

39 C. F. Thurston, The structure and function of fungal laccases, *Microbiology*, 1994, **140**, 19–26.

40 J. A. Buswell and K.-E. L. Eriksson, Effect of lignin-related phenols and their methylated derivatives on the growth of eight white-rot fungi, *World J. Microbiol. Biotechnol.*, 1994, **10**, 169–174.

41 X. He, D. C. Sorescu and A. Star, Composition and structure of fluorescent graphene quantum dots generated by enzymatic degradation of graphene oxide, *J. Phys. Chem. C*, 2021, **125**, 13361–13369.

42 J. K. Dittmer, N. J. Patel, S. W. Dhawale and S. S. Dhawale, Production of multiple laccase isoforms by *Phanerochaete chryosporium* grown under nutrient sufficiency, *FEMS Microbiol. Lett.*, 1997, **149**, 65–70.

43 A. Piscitelli, P. Giardina, V. Lettera, C. Pezzella, G. Sannia and V. Faraco, Induction and transcriptional regulation of laccases in fungi, *Curr. Genomics*, 2011, **12**, 104–112.

44 A. Leonowicz, N. Cho, J. Luterek, A. Wilkolazka, M. Wojtas-Wasilewska, A. Matuszewska, M. Hofrichter, D. Wesenberg and J. Rogalski, Fungal laccase: Properties and activity on lignin, *J. Basic Microbiol.*, 2001, **41**, 185–227.

45 Y. Zhao, B. L. Allen and A. Star, Enzymatic degradation of multiwalled carbon nanotubes, *J. Phys. Chem. A*, 2011, **115**, 9536–9544.

46 W. Xing, G. Lalwani, I. Rusakova and B. Sitharaman, Degradation of graphene by hydrogen peroxide, *Part. Part. Syst. Charact.*, 2014, **31**, 745–750.

47 S. P. Mukherjee, A. R. Gliga, B. Lazzaretto, B. Brandner, M. Fielden, C. Vogt, L. Newman, A. F. Rodrigues, W. Shao, P. M. Fournier, M. S. Toprak, A. Star, K. Kostarelos, K. Bhattacharya and B. Fadeel, Graphene oxide is degraded by neutrophils and the degradation products are non-genotoxic, *Nanoscale*, 2018, **10**, 1180–1188.

48 J.-H. Chen, W. G. Cullen, C. Jang, M. S. Fuhrer and E. D. Williams, Defect scattering in graphene, *Phys. Rev. Lett.*, 2009, **102**, 236805.
49 A. Jorio, E. H. M. Ferreira, M. V. O. Moutinho, F. Stavale, C. A. Achete and R. B. Capaz, Measuring disorder in graphene with the G and D bands, *Phys. Status Solidi B*, 2010, **247**, 2980–2982.
50 A. O. Falade, U. U. Nwodo, B. C. Iweriebor, E. Green, L. V. Mabinya and A. I. Okoh, Lignin peroxidase functionalities and prospective applications, *MicrobiologyOpen*, 2017, **6**, e00394.
51 A. K. Singh, M. Bilal, H. M. N. Iqbal and A. Raj, Lignin peroxidase in focus for catalytic elimination of contaminants — A critical review on recent progress and perspectives, *Int. J. Biol. Macromol.*, 2021, **177**, 58–82.
52 B. D. Faison and T. K. Kirk, Factors involved in the regulation of a ligninase activity in *Phanerochaete chrysosporium*, *Appl. Environ. Microbiol.*, 1985, **49**, 299–304.
53 D. Singh and S. Chen, The white-rot fungus *Phanerochaete chrysosporium*: Conditions for the production of lignin-degrading enzymes, *Appl. Microbiol. Biotechnol.*, 2008, **81**, 399–417.
54 J. Zhang, F. Zhang, H. Yang, X. Huang, H. Liu, J. Zhang and S. Guo, Graphene oxide as a matrix for enzyme immobilization, *Langmuir*, 2010, **26**, 6083–6085.
55 A. G. Olabi, T. Wilberforce, E. T. Sayed, K. Elsaid, H. Rezk and M. A. Abdelkareem, Recent progress of graphene based nanomaterials in bioelectrochemical systems, *Sci. Total Environ.*, 2020, **749**, 141225.
56 M. De, S. S. Chou and V. P. Dravid, Graphene oxide as an enzyme inhibitor: modulation of activity of α-chymotrypsin, *J. Am. Chem. Soc.*, 2011, **133**, 17524–17527.
57 I. V. Pavlidis, T. Vorhaben, D. Gournis, G. K. Papadopoulos, U. T. Bornscheuer and H. Stamatis, Regulation of catalytic behaviour of hydrolases through interactions with functionalized carbon-based nanomaterials, *J. Nanopart. Res.*, 2012, **14**, 842.
58 A. A. Vertegel, R. W. Siegel and J. S. Dordick, Silica nanoparticle size influences the structure and enzymatic activity of adsorbed lysozyme, *Langmuir*, 2004, **20**, 6800–6807.
59 T. Glumoff, P. J. Harvey, S. Molinari, M. Goble, G. Frank, J. M. Palmer, J. D. G. Smit and M. S. A. Leisola, Lignin peroxidase from *Phanerochaete chrysosporium* molecular and kinetic characterization of isozymes, *Eur. J. Biochem.*, 1990, **187**, 515–520.
60 J. Pérez, J. Martínez and T. De La Rubia, Purification and partial characterization of a laccase from the white rot fungus *Phanerochaete flavido-alba*, *Appl. Environ. Microbiol.*, 1996, **62**, 4263–4267.
61 X. Hu, Y. Yu, Y. Wang, J. Zhou and L. Song, Separating nano graphene oxide from the residual strong-acid filtrate of the modified Hummers method with alkaline solution, *Appl. Surf. Sci.*, 2015, **329**, 83–86.
62 Y. Chen, Z. Luo and X. Lu, Construction of novel enzyme–graphene oxide catalytic interface with improved enzymatic performance and its sssembly mechanism, *ACS Appl. Mater. Interfaces*, 2019, **11**, 11349–11359.
63 D. Kishore, M. Talat, O. N. Srivastava and A. M. Kayastha, Immobilization of β-galactosidase onto functionalized graphene nano-sheets using response surface methodology and its analytical applications, *PLoS One*, 2012, **7**, e40708.
64 A. A. Dias, R. M. Bezerra, P. M. Lemos and A. Nazaré Pereira, In vivo and laccase-catalysed decolourization of xenobiotic azo dyes by a basidiomycetous fungus: characterization of its ligninolytic system, *World J. Microbiol. Biotechnol.*, 2003, **19**, 969–975.
65 L. Kupski, G. M. Salcedo, S. S. Caldas, T. D. de Souza, E. B. Furlong and E. G. Primel, Optimization of a laccase-mediator system with natural redox-mediating compounds for pesticide removal, *Environ. Sci. Pollut. Res.*, 2019, **26**, 5131–5139.
66 R. Hilgers, G. Van Erven, V. Boerkamp, I. Sulaeva, A. Potthast, M. A. Kabel and J. P. Vincken, Understanding laccase/HBT-catalyzed grass delignification at the molecular level, *Green Chem.*, 2020, **22**, 1735–1746.
67 E. I. Solomon, A. J. Augustine and J. Yoon, O_2 Reduction to H2O by the multicopper oxidases, *Dalton Trans.*, 2008, 3921–3932.
68 V. Perna, A. S. Meyer, J. Holck, L. D. Eltis, V. G. H. Eijsink and J. Wittrup Agger, Laccase-Catalyzed oxidation of lignin induces production of H_2O_2, *ACS Sustain. Chem. Eng.*, 2020, **8**, 831–841.
69 E. Srebotnik and J. N. Boisson, Peroxidation of linoleic acid during the oxidation of phenols by fungal laccase, *Enzyme Microb. Technol.*, 2005, **36**, 785–789.
70 P. Giardina, V. Faraco, C. Pezzella, A. Piscitelli, S. Vanhulle and G. Sannia, Laccases: A never-ending story, *Cell. Mol. Life Sci.*, 2010, **67**, 369–385.
71 *Graphenea*, 2021a, **https://www.graphenea.com/collections/graphene-oxide/products/graphene-oxide-4-mg-ml-water-dispersion-1000-ml**, [Accessed December 13, 2022].
72 *Graphenea*, 2021b, **https://www.graphenea.com/products/reduced-graphene-oxide-1-gram**, [Accessed December 13, 2022].

